Heat Transport along a Vertical Sheet with Induced Magnetic Field: A Transient Approach

Md. Asaduzzaman Department of CSE North Western University Khulna, Bangladesh spandan.ku@gmail.com Mahamudul Hassan Milon
Department of CSE
North Western University
Khulna, Bangladesh
mahamudulmilon@yahoo.com

Abstract— The effect of thermal diffusion on the magneto-hydrodynamic heat transfer in an unsteady flow past a sheet perpendicular to the horizontal is a significant aspect in many engineering applications. It has been investigated numerically under the action of a strong induced magnetic field. This approach is used for solving cooling problems involving lighter and heavier particles. Numerical solutions for the velocity, induced magnetic field, and temperature are obtained for associated parameters using the explicit finite difference method. The obtained results are illustrated in graphs using the programming language named Fortran, followed by the software Techplot, to observe the effects of various parameters like Grashof number, Prandtl number, and Eckert number on the corresponding quantities. Finally, the outcomes of the approach are concluded.

Keywords—MHD, Transient heat Transfer, Induced Magnetic Field.

I. INTRODUCTION

Alfven [1] first explained the abstraction of MHD. As per the abstraction, "if a conducting liquid is placed in a constant magnetic field, every motion of the liquid gives rise to an electromagnetic force that produces electric currents. Owing to the magnetic field, these currents give mechanical forces that change the state of motion of the liquid. Thus, a kind of combined electromagnetic-hydrodynamic wave is produced." Heat transfer plays a significant role in fluids condensing or boiling at a solid surface. consideration arises due to buoyancy forces caused by thermal diffusions. For isothermal system the heat transfer aling a vertical plate has been observed by Callahan and Marner [2]. [3] Chaudhary and Sharma (2006) have analytically analyzed the combined heat and mass transfer flow with induced magnetic field. [4] Chen have observed the MHD combined heat and mass transfer in natural convection adjacent to a vertical surface. There are analytical solution restrictions in their studies. Condensing and boiling are characteristic for many separation processes in chemical engineering as drying, evaporation, distillation, condensation, rectification and absorption of a fluid. [5] Pera and Gebhart was first author to investigate the combined buoyancy effects of thermal and mass diffusions on natural convection flow. Labrosse [6] conceptualized

as well as experimented the Soret effect for thermogravitational column and obtained a good impact. Gokhale and Soundalgekar [7] considered the constant heat flux to investigate the unsteady free convection for MHD. In the presence of pressure gradient, the MHD boundary layer has been caried out by Gribben [8]. [9] Lin and Wu have studied simultaneous heat and mass transfer model with the entire range of buoyancy ratio for most practical chemical species in dilute and aqueous solutions. There are many individuals [10, 12, 13, 14, 15, 16, 17] who investigated the impacts of heat transfer and corresponding findinas. concluded their reference these studies, the effect of thermal diffusion on MHD free convection and mass transfer flows have also been considered by many investigators due to its important role particularly in isotope separation and in mixtures between gases with very light molecular weight (H_2, H_2) and medium molecular weight (N_2, H_2) air) (Eckert and Drake, 1972). Recently, [11] Alam et al. have numerically investigated the mass transfer flow past a vertical permeable medium with heat generation and thermal diffusion on the combined free-forced convection under the transversely applied magnetic field. In all the papers cited earlier, the studies concentrated on MHD free convection and mass transfer flow of incompressible viscous fluid past a continuously moving surface under only the action of transverse magnetic field with or without thermal diffusion. But the flow under the action of a strong magnetic field that induced another magnetic field have of great interest in geophysics and astrophysics. A numerical study of steady combined heat and mass transfer by mixed convection flow past a continuously moving infinite vertical porous plate under the action of strong magnetic field with constant suction velocity, constant heat and mass fluxes have been investigated by [11] Alam et. al. For unsteady two-dimensional case, the above problem becomes more complicated. These types of problems play a special role in nature, in many separation processes as isotope separation, in between gases, in many applications as solidification of binary alloy as well as in astrophysical and geophysical engineering. The goal of the existing research is to examine the unsteady heat transport with induced magnetic field along a vertical semi-infinite plate.

II. MATHEMATICAL MODEL

Transient MHD heat transfer of an electrically conducting incompressible viscous fluid past an electrically non-conducting continuously moving semiinfinite vertical plate with thermal diffusion is modeled here. In Cartesian coordinate system, the x-axis is chosen along the plate in the direction of flow and the y-axis is normal to it. Normal to the flow region strong uniform magnetic field is sued. Because of the magnetic Reynolds number, the flow is not taken to be small enough, the induced magnetic field is not negligible and is of the form $(H_x, H_y, 0)$.

The divergence equation $\nabla \cdot \mathbf{H} = 0$ of Maxwell's equation for the magnetic field gives $H_{\nu} = H_0$.

Initially we chose that the plate as well as the fluid are at the same temperature $T(=T_{\infty})$ everywhere in the fluid is same. Also, it is claimed that the fluid and the plate is at rest after that the plate is to be moving with a constant velocity U_0 in its own plane and instantaneously at time T > 0, the temperature of the plate is raised to $T(>T_{\infty})$, which is thereafter maintained constant, where T_w is the temperature at the wall and T_{∞} is the temperature of the species far away from the plate respectively. The physical model of this study is furnished in the following figure.

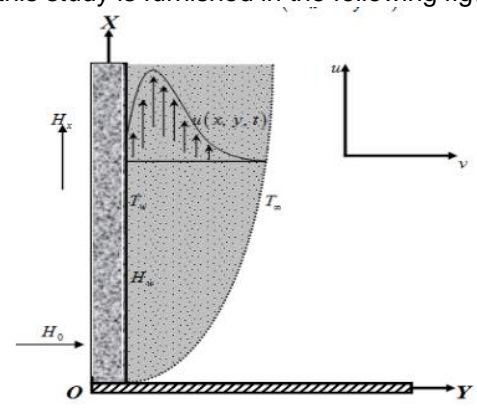


Figure 1: Physical configuration [11]

Also, the study is based on the following abstractions:

i. All the physical properties of the fluid are considered to be constant except the influence of variations of density with temperature are considered only on the body force term, in accordance with the Boussinesq's approximation.

ii. There is no chemical reaction taking place between the foreign mass and the fluid.

iii. The equation of conservation of electric charge, $\nabla J = 0$ gives $J_{\nu} = \text{constant}$ where the current density $J = (J_x, J_y, J_z)$, because the direction of propagation is considered only along the y-axis and J does not have any variation along the y-axis. Since the plate is electrically non-conducting, the constant is zero i.e. $J_{v} = 0$ at the plate and everywhere.

Continuity equation
$$\frac{\partial u}{\partial x} + \frac{\partial v}{\partial y} = 0 \tag{1}$$

Momentum equation

$$\begin{split} \frac{\partial u}{\partial t} + u \frac{\partial u}{\partial x} + v \frac{\partial u}{\partial y} &= v \frac{\partial^2 u}{\partial y^2} + g\beta(T - T_{\infty}) + g\beta^*(C - C_{\infty})\cos\gamma - \frac{\mu_e}{\rho} H_0 \frac{\partial H_x}{\partial y} - \frac{v}{k_I} u \end{split} \tag{2}$$

Magnetic Induction Equation
$$\frac{\partial H_x}{\partial t} + u \frac{\partial H_x}{\partial x} + v \frac{\partial H_x}{\partial y} = H_x \frac{\partial u}{\partial x} + H_0 \frac{\partial u}{\partial y} + \frac{1}{\sigma \mu_e} \frac{\partial^2 H_x}{\partial y^2}$$
 (3) Energy equation

$$\frac{\partial T}{\partial t} + u \frac{\partial T}{\partial x} + v \frac{\partial T}{\partial y} = \frac{k}{\rho c_p} \frac{\partial^2 T}{\partial y^2} + \frac{1}{\rho c_p \sigma} \left(\frac{\partial H_x}{\partial y}\right)^2 + \frac{v}{c_p} \left(\frac{\partial u}{\partial y}\right)^2 \tag{4}$$

with the corresponding initial and boundary conditions

$$t = 0, u = 0, v = 0, H_x = 0, T \to T_{\infty} \text{ at everywhere (5)}$$

$$u = 0, v = 0, H_x = 0, T \to T_{\infty} \text{ at } x = 0$$

$$t > 0, \begin{cases} u = 0, v = 0, H_x = H_w, T = T_w \text{ at } y = 0 \\ u = 0, v = 0, H_x = 0, T \to T_{\infty} \text{ as } y \to \infty \end{cases}$$
(6)

where x, y are Cartesian coordinate system; u, v are x, y component of flow velocity respectively; g is the local acceleration due to gravity; β is the thermal expansion coefficient; u is the kinematic viscosity; μ_e is the magnetic permeability; ρ is the density of the fluid; H_0 is the constant induced magnetic field; H_x be the x -component induced magnetic field; σ is the electrical conductivity; κ is the thermal conductivity; \mathcal{C}_{p} is the specific heat at the constant pressure and H_w is the induced magnetic field at the wall.

Upon introducing the dimensionless quantities

$$X = \frac{xU_0}{v}, \quad Y = \frac{yU_0}{v}, \quad U = \frac{u}{U_0}, \quad V = \frac{v}{U_0}, \quad \tau = \frac{tU_0^2}{v},$$

$$\overline{H_X} = \frac{\sqrt{\frac{\mu_e}{\rho}} H_X}{U_0}, \quad \overline{T} = \frac{(T - T_{\infty})}{T_W - T_{\infty}}$$

The above equations from (1) to (4) have the new shapes as follows:

(7)

(9)

17823

$$\frac{\partial U}{\partial x} + \frac{\partial V}{\partial y} = 0$$

$$\frac{\partial U}{\partial \tau} + U \frac{\partial U}{\partial X} + V \frac{\partial U}{\partial Y} = G_r \overline{T} + \frac{\partial^2 U}{\partial Y^2} + M \frac{\partial \overline{H_X}}{\partial Y} + \kappa U$$
(8)

$$\frac{\partial \overline{H_X}}{\partial \tau} + U \frac{\partial \overline{H_X}}{\partial X} + V \frac{\partial \overline{H_X}}{\partial Y} = \overline{H_X} \frac{\partial U}{\partial X} + M \frac{\partial U}{\partial Y} + \frac{1}{P_m} \frac{\partial^2 \overline{H_X}}{\partial Y^2}$$

$$\frac{\partial \overline{T}}{\partial \tau} + U \frac{\partial \overline{T}}{\partial x} + V \frac{\partial \overline{T}}{\partial Y} = \frac{E_c}{P_m} \left(\frac{\partial \overline{H_X}}{\partial Y} \right)^2 + E_c \left(\frac{\partial U}{\partial Y} \right)^2 + \frac{1}{P_r} \frac{\partial^2 \overline{T}}{\partial Y^2}$$
 (10) where, $G_r = \frac{vg\beta(T_W - T_\infty)}{U_0^3}$ (Grashof number),

$$M = \frac{H_0}{U_0} \sqrt{\frac{\mu_e}{\rho}}$$
 (Magnetic Force Number),

 $P_m = v\sigma'\mu_e$ (Magnetic diffusivity Number),

$$P_r = \frac{v \, \rho C_p}{\kappa} \, \text{(Prandtl Number)},$$

$$E_c = \frac{U_0^2}{c_p(T_w - T_\infty)} \, \text{(Eckert Number) and } \kappa = \frac{v^2}{\kappa \cdot U_0^2}$$

with the corresponding boundary conditions

$$\tau = 0, U = 0, V = 0, \overline{H_x} = 0, \overline{T} = 0 \text{ at everywhere } (11)$$

$$\begin{cases} U = 0, V = 0, \overline{H_x} = 0, \overline{T} = 0 \text{ at } X = 0 \end{cases}$$

$$\tau > 0, \begin{cases} U = 0, V = 0, \overline{H_x} = 0, \overline{T} = 0 \text{ at } X = 0 \\ U = 0, V = 0, \overline{H_x} = 1, \overline{T} = 1 \text{ at } Y = 0 \\ U = 0, V = 0, \overline{H_x} = 0, \overline{T} = 0 \text{ as } y \to \infty \end{cases}$$
 (12)

The explicit finite difference method has been used to solve equations (7) to (10) subject to the conditions given by (11) and (12). Here we have,

$$\frac{\vec{y}_{i,j} - u_{i-1,j}}{\Delta X} + \frac{v_{i,j} - v_{i-1,j}}{\Delta Y} = 0$$
 (13)

$$\frac{U'_{i,j}-U_{i,j}}{\Delta \tau} + U_{i,j} \frac{U_{i,j}-U_{i-1,j}}{\Delta X} + V_{i,j} \frac{U_{i,j}-U_{i-1,j}}{\Delta Y} = G_r \bar{T}_{i,j} + U_{i,j} \frac{U_{i,j-1}-I_{i,j}}{\Delta Y} + KU_{i,j} \qquad (14)$$

$$\frac{U_{i,j+1}-2U_{i,j}+U_{i,j-1}}{(\Delta Y)^2} + M \frac{\bar{H}_{x_{i,j+1}}-\bar{H}_{x_{i,j}}}{\Delta Y} + KU_{i,j} \qquad (14)$$

$$\frac{\bar{H}_{x_{i,j}}-\bar{H}_{x_{i,j}}}{\Delta \tau} + U_{i,j} \frac{\bar{H}_{x_{i,j}}-\bar{H}_{x_{i-1,j}}}{\Delta X} + V_{i,j} \frac{\bar{H}_{x_{i,j+1}}-\bar{H}_{x_{i,j}}}{\Delta Y} = \bar{H}_{x_{i,j}} \frac{U_{i,j-1}-U_{i-1,j}}{\Delta X} + M \frac{U_{i,j+1}-U_{i,j}}{\Delta Y} + \frac{1}{P_m} \frac{\bar{H}_{x_{i,j+1}}-2\bar{H}_{x_{i,j}}+\bar{H}_{x_{i,j-1}}}{(\Delta Y)^2}$$

$$\frac{\bar{T}_{i,j}-\bar{T}_{i,j}}{\Delta \tau} + U_{i,j} \frac{\bar{T}_{i,j}-\bar{T}_{i-1,j}}{\Delta X} + V_{i,j} \frac{\bar{T}_{i,j+1}-\bar{T}_{i,j}}{\Delta Y} = \bar{T}_{i,j} = \bar{T}_{i,j}$$

$$\frac{\overline{T_{i,j}} - \overline{T}_{i,j}}{\Delta \tau} + U_{i,j} \frac{\overline{T}_{i,j} - \overline{T}_{i-1,j}}{\Delta X} + V_{i,j} \frac{\overline{T}_{i,j+1} - \overline{T}_{i,j}}{\Delta Y} = \frac{1}{P_r} \frac{\overline{T}_{i,j+1} - 2\overline{T}_{i,j} + \overline{T}_{i,j-1}}{(\Delta Y)^2} + \frac{E_c}{P_m} \left(\frac{\overline{H}_{X_{i,j+1}} - \overline{H}_{X_{i,j}}}{\Delta Y}\right)^2 + E_c \left(\frac{U_{i,j+1} - U_{i,j}}{\Delta Y}\right)^2 \tag{16}$$

and the initial and boundary conditions with the finite difference scheme are

$$U^{0}_{i,j} = 0, V^{0}_{i,j} = 0, \overline{H}^{0}_{x_{i,j}} = 0, \overline{T}^{0}_{i,j} = 0$$

$$U^{0}_{i,j} = 0, V^{0}_{i,j} = 0, \overline{T}^{0}_{i,j} = 0$$

$$U^{0}_{i,j} = 0, V^{0}_{i,j} = 0, \overline{T}^{0}_{i,j} = 0, \overline{T}^{0}_{i,j} = 0$$

$$U^{0}_{i,j} = 0, V^{0}_{i,j} = 0, \overline{T}^{0}_{i,j} = 0, \overline{T}^{0}_{i,j} = 0$$

$$U^{0}_{i,j} = 0, V^{0}_{i,j} = 0, \overline{T}^{0}_{i,j} = 0, \overline{T}^{0}_{i,j} = 0$$

$$U^{0}_{i,j} = 0, \overline{T}^{0}_{i,j} = 0, \overline{T}^{0}_{i,j} = 0, \overline{T}^{0}_{i,j} = 0, \overline{T}^{0}_{i,j} = 0$$

$$U^{0}_{i,j} = 0, \overline{T}^{0}_{i,j} = 0, \overline{T}^{0}_{i,j} = 0, \overline{T}^{0}_{i,j} = 0, \overline{T}^{0}_{i,j} = 0$$

$$U^{n}_{0,j} = 0, V^{n}_{0,j} = 0, \overline{H}^{n}_{x_{0,j}} = 0, \overline{T}^{n}_{0,j} = 0$$

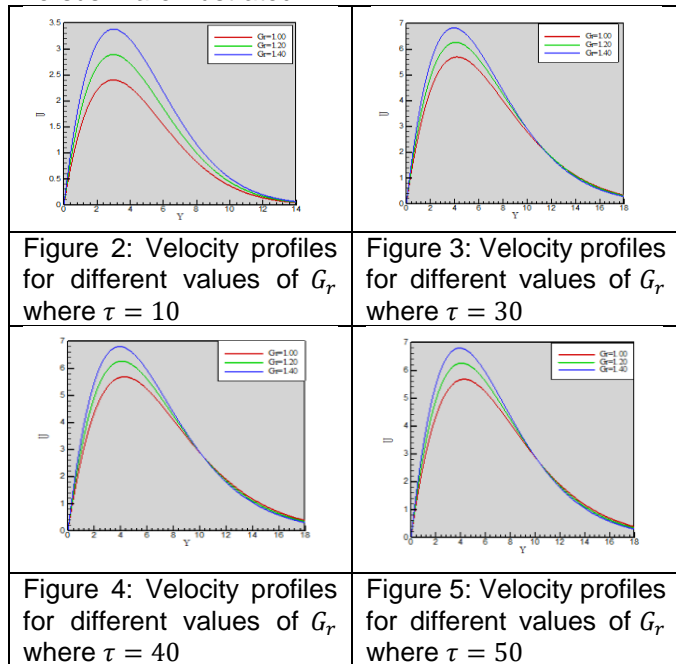
$$U^{n}_{i,0} = 0, V^{n}_{i,0} = 0, \overline{H}^{n}_{x_{i,0}} = 1, \overline{T}^{n}_{i,0} = 1$$
 (18)

 $U^{n}{}_{i,L} = 0, V^{n}{}_{i,L} = 0, \overline{H}^{n}{}_{x_{i,L}} = 0, \overline{T}^{n}{}_{i,L} = 0$ Where $L \to \infty$.

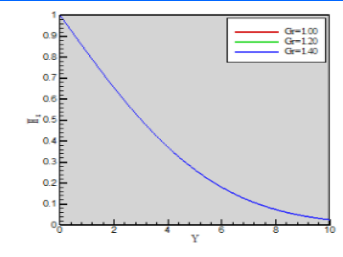
Here the subscripts i and j designate the grid points with x and y coordinates respectively and the superscript n represents a value of time, $\tau = n \Delta \tau$ where n = 0, 1, 2, ...

III. RESULTS AND DISCUSSIONS

Along with the obtained steady state solutions, the flow behaviors in case of cooling problem are discussed graphically. The profiles of the transient velocity, induced magnetic field and temperature versus Y are illustrated.



For the change of G_r , the velocity profile is shown in (Figures 2 to 5). From these Figures we see that, as the value of G_r increases the velocity profile also increases at T =10, 30 and 40. But at T =50 the velocity profile shows same graph as $\tau = 40$.



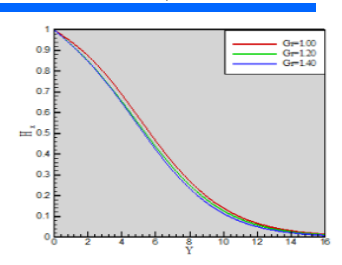
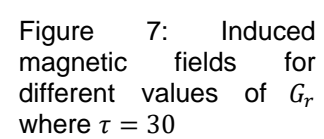
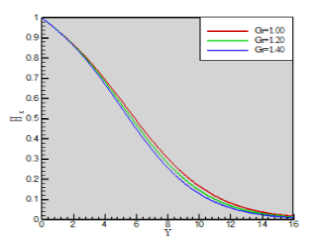


Figure 6: Induced magnetic fields for different values of G_r where $\tau = 10$





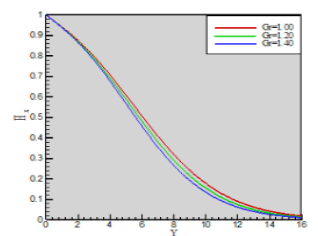
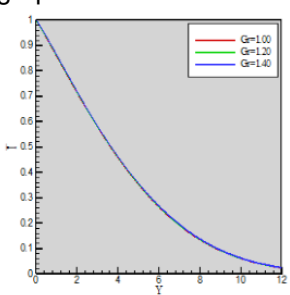


Figure 8: Induced magnetic fields for different values of G_r where $\tau = 40$

9: **Figure** Induced magnetic fields different values of G_r where $\tau = 50$

The induced magnetic field profile (Figures 6 to 9) remains same as the value of G_r increases at τ =10. But for τ =30, 40 and 50 the induced magnetic field profile decreases as the value of G_r increases. At τ =50 the induced magnetic field profile shows identical graph as $\tau = 40$.



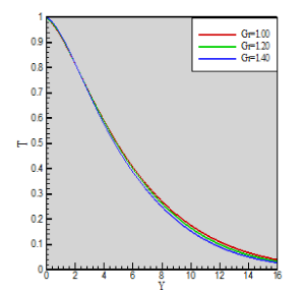
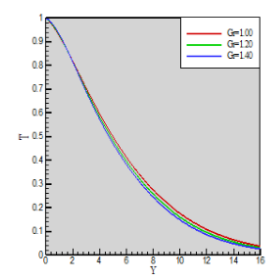


Figure 10: Temperature profiles for different values of G_r where $\tau = 10$

Figure 11: Temperature profiles for different of G_r values where



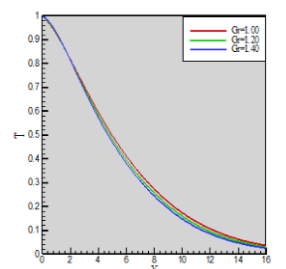
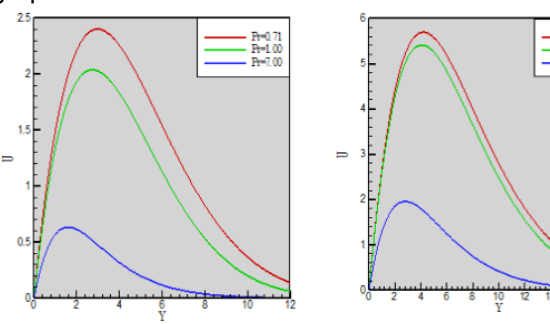


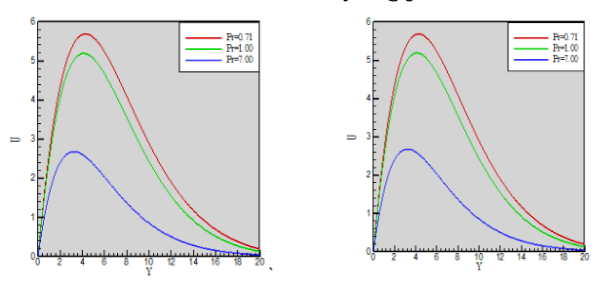
Figure 12: Temperature profiles for different values of G_r where $\tau = 40$

Figure 13: Temperature profiles for different of G_r values where $\tau = 50$

The temperature profile (Figs. 10 to 13) remains same as the value of G_r increases at τ =10. But for τ =30, 40 and 50 the temperature profile decreases as the value of G_r increases. At τ =50 the temperature profile shows identical graph as τ =40. Also as the value of τ increases the temperature profiles increase upto τ =40. But at τ =50 the temperature profile shows same graph as τ =40.



15: **Figure** 14: Velocity **Figure** Velocity different different profiles for profiles for values of P_r where $\tau = 10$ values of P_r where $\tau = 30$



16: 17: Figure Velocity Figure Velocity profiles for different profiles for different values of P_r where $\tau = 40$ values of P_r where $\tau = 50$

As the value of Pr increases the velocity profile (Figs. 14 to 17) decreases at τ =10, 30 and 40. But at τ =50 the velocity profile shows same graph as τ =40. One the other hand, as the value of τ increases the velocity profiles also increase upto τ =40. But at τ =50 the velocity profile shows same graph as τ =40.

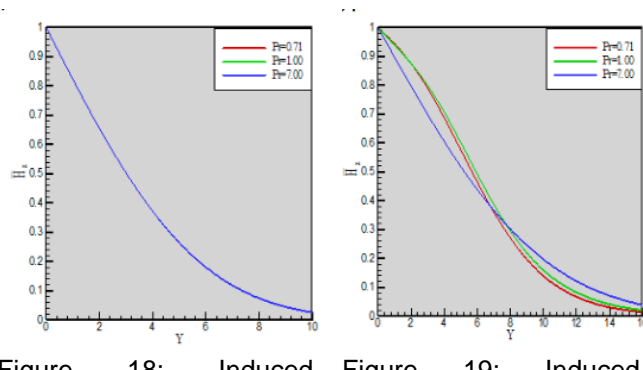


Figure Induced **Figure** 19: Induced magnetic magnetic fields fields for for different values different values of P_r of P_r where $\tau = 10$ where $\tau = 30$

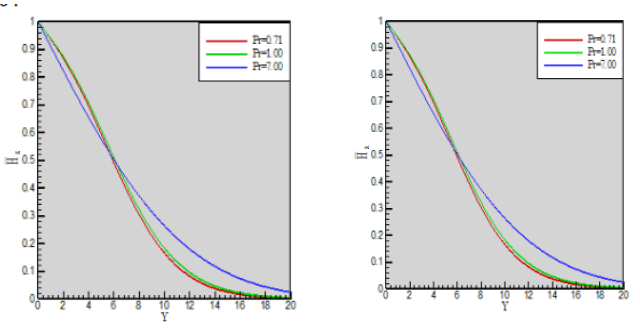


Figure 20: Induced **Figure** 21: Induced magnetic fields for magnetic fields for different values of P_r different values of P_r where $\tau = 40$ where $\tau = 50$

The induced magnetic field profile (Figs. 18 to 21) remains same as the value of Pr increases at τ =10. But for τ =30, 40 and 50 the induced magnetic field profile initially decreases and after certain amount of Y it increases as the value of Pr increases. At τ =50 the induced magnetic field profile shows identical graph as τ =40. Also as the value of τ increases the induced magnetic field profiles also increase upto τ =40. But at τ =50 the induced magnetic field profile shows same graph as τ =40.

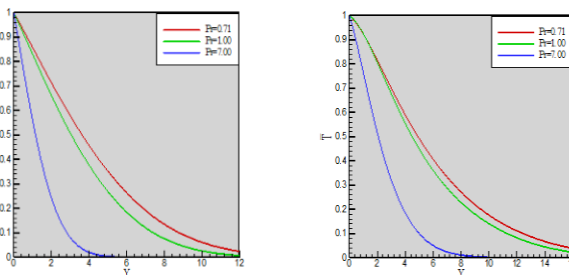


Figure 22: Temperature Figure 23: Temperature profiles for different profiles for different values of P_r where $\tau=10$ values of P_r where $\tau=30$

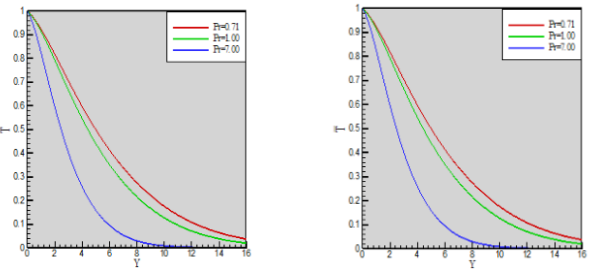
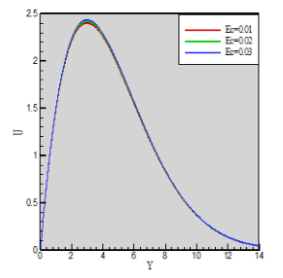


Figure 24: Temperature Figure 25: Temperature profiles for different profiles for different values of P_r where $\tau=40$ values of P_r where $\tau=50$

As the value of Pr increases the temperature profile (Figs. 22 to 25) decreases at τ =10, 30 and 40. But at τ =50 the temperature profile shows same graph as τ =40. One the other hand, as the value of τ inc reases the temperature profiles also increase upto τ =40. But at τ =50 the temperature profile shows same graph as τ =40.



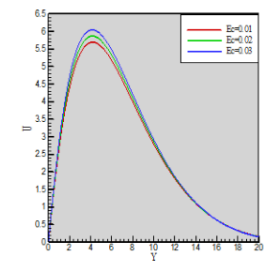
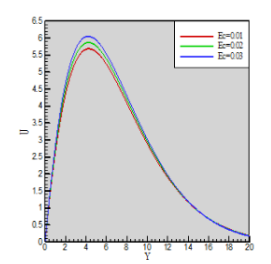


Figure 26: Velocity profiles for different values of E_c where $\tau=10$

Figure 27: Velocity profiles for different values of E_c where $\tau=30$



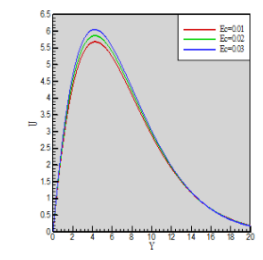
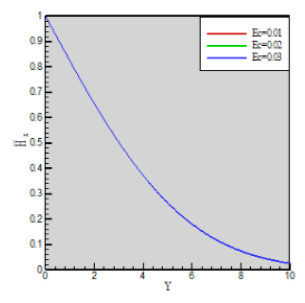


Figure 28: Velocity profiles for different values of E_c where $\tau=40$

Figure 29: Velocity profiles for different values of E_c where $\tau = 50$

As the value of E_c increases the velocity profile (Figs. 26 to 29) also increases at τ =10, 30 and 40. But at τ =50 the velocity profile shows same graph as τ =40. One the other hand, as the value of τ increases the velocity profiles also increase upto τ =40. But at τ =50 the velocity profile shows same graph as τ =40.



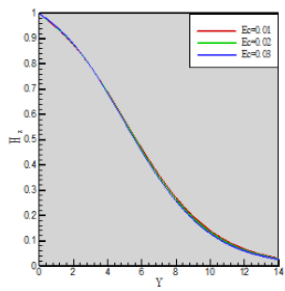
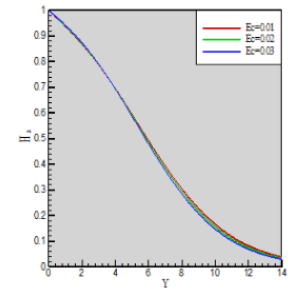


Figure 30: Induced magnetic fields for different values of E_c where $\tau=10$

Figure 31: Induced magnetic fields for different values of E_c where $\tau=30$



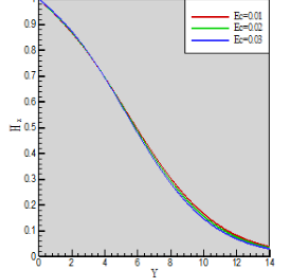
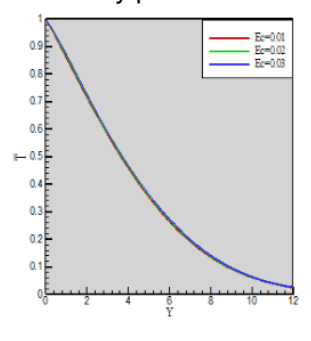


Figure 32: Induced magnetic fields for different values of E_c where $\tau=40$

Figure 33: Induced magnetic fields for different values of E_c where $\tau=50$

The induced magnetic field profile (Figs. 30 to 33) remains same as the value of E_c increases at τ =10. But for τ =30, 40 and 50 the induced magnetic field profile decreases as the value of cE increases. At τ =50 the induced magnetic field profile shows identical graph as τ =40. Also as the value of τ increases the velocity profiles also increase upto τ =40. But at τ =50 the velocity profile shows same graph as τ =40.



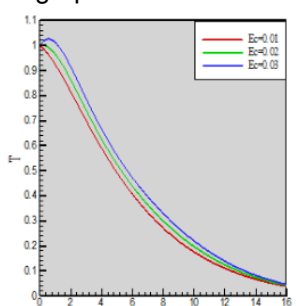
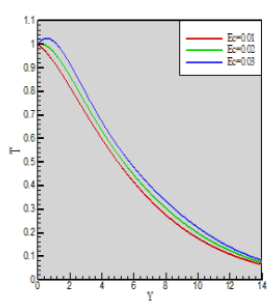


Figure 34: Temperature profiles for different values of E_c where $\tau = 10$

Figure 35: Temperature profiles for different values of E_c where $\tau = 30$



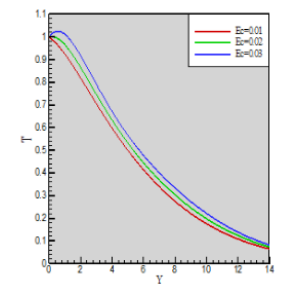


Figure 36: Temperature profiles for different values of E_c where $\tau = 40$

Figure 37: Temperature profiles for different values of E_c where $\tau = 50$

As the value of E_c increases the temperature profile (Figs. 34 to 37) increases at τ =10, 30 and 40. But at τ =50 the temperature profile shows same graph as τ =40. One the other hand, as the value of τ increases the temperature profiles also increase upto τ =40. But at τ =50 the temperature profile shows same graph as τ =40.

IV. CONCLUSIONS

An unsteady heat transfer flow through an electrically conducting incompressible viscous fluid past along an electrically nonconducting semi-infinite vertical plate under the action of strong magnetic field taking into account this approach. The resulting governing system of dimensionless coupled non-linear PDE's are numerically solved by an explicit finite difference method. The results are discussed for different values of important numbers as magnetic parameter, magnetic diffusivity numbers, Grashof number, Prandtl number and Eckert number. Some of the important findings obtained from the graphical representation of the results are listed herewith;

- 1. The velocity improves with the rises of E_c or lift down with the uplifting values of P_r .
- 2. The magnetic induction downgrades with the upgrades of G_r , E_c . Moreover, the magnetic induction initially reduces and later increases with the advancement of P_r . Particularly, for heavier particles the induced magnetic field is greater than the lighter particles.
- 3. The temperature soars with the climb of E_c while it falls with the climb of G_r or P_r . Particularly, the fluid temperature is more for air than water and it is less for lighter than heavier particles.

As the basis for many scientific and engineering applications for studying more complex vertical problems involving the flow of electrically conducting fluids, it is hoped that the present investigation of the study of applied physics of flow over a vertical surface can be utilized. In the migration of underground water or oil as well as in the filtration and water purification processes, the findings may be useful for study of movement of oil or gas and water through the reservoir of an oil or gas field. The results of the problem are also of great interest in geophysics and astrophysics in the study of interaction of the geomagnetic field with the fluid in geothermal region.

REFERENCES

- [1] Alfvén, H. (1942). Existence of electromagnetic-hydrodynamic waves. *Nature*, *150*(3805), 405-406.
- [2] Callahan, G. D., & Marner, W. J. (1976). Transient free convection with mass transfer on an isothermal vertical flat plate. *International Journal of Heat and Mass Transfer*, 19(2), 165-174.
- [3] Chaudhary, R. C., & Sharma, B. K. (2006). Combined heat and mass transfer by laminar mixed convection flow from a vertical surface with induced magnetic field. *Journal of Applied Physics*, 99(3).
- [4] Chen, C. H. (2004). Combined heat and mass transfer in MHD free convection from a vertical surface with Ohmic heating and viscous dissipation. *International journal of engineering science*, 42(7), 699-713.
- [5] Gebhart, B. and Pera, L.(1971), "Combined buoyancy effects of thermal and mass diffusions on natural convection flow", *Int. J. Heat Mass Transfer*,14, 2026.
- [6] Labrosse, G. (2003). Free convection of binary liquid with variable Soret coefficient in thermogravitational column: The steady parallel base states. *Physics of Fluids*, *15*(9), 2694-2727.
- [7] Gokhale, M. Y., & Soundalgekar, V. M. (1991). Magnetohydrodynamic transient-free convection flow past a semi-infinite vertical plate with constant heat flux. *Canadian journal of physics*, 69(12), 1451-1453.
- [8] Gribben, R. J. (1965). The magnetohydrodynamic boundary layer in the presence of a pressure gradient. *Proceedings of the Royal Society of London. Series A. Mathematical and Physical Sciences*, 287(1408), 123-141.
- [9] Lin, H. T., & Wu, C. M. (1997). Combined heat and

- mass transfer by laminar natural convection from a vertical plate with uniform heat flux and concentration. *Heat and Mass Transfer*, 32(4), 293-299.
- [10] Michael Faraday, (1832) "Electromagnetic Force Field, Particle/Field Duality" 2, 525-1333,.
- [11] Alam, M. M., Islam, M. R., & Rahman, F. (2008). Study heat and mass transfer by mixed convection flow from a vertical porous plate with induced magnetic field, constant heat and mass fluxes. *Science & technology asia*, 1-13.
- [12] Muthukumaraswamy, R., & Ganesan, P. (1998). Unsteady flow past an impulsively started vertical plate with heat and mass transfer. *Heat and Mass transfer*, *34*(2), 187-193.
- [13] Ostrach, S. (1952). An analysis of laminar freeconvection flow and heat transfer about a flat plate parallel to the direction of the generating body force (No. NACATN2635).
- [14] PEDDIESON, J. (1970). BOUNDARY LAYER THEORY FOR A MICROPOLAR FLUID.
- [15] Tsou, F. K., Sparrow, E. M., & Goldstein, R. J. (1967). Flow and heat transfer in the boundary layer on a continuous moving surface. *International Journal of Heat and Mass Transfer*, 10(2), 219-235.
- [16] Soundalgekar, V. M., & Ganesan, P. (1981). Finite-difference analysis of transient free convection with mass transfer on an isothermal vertical flat plate. *International Journal of Engineering Science*, 19(6), 757-770.
- [17] Takhar, H. S., Ganesan, P., Ekambavanan, K., & Soundalgekar, V. M. (1997). Transient free convection past a semi-infinite vertical plate with variable surface temperature. *International Journal of Numerical Methods for Heat & Fluid Flow*, 7(4), 280-296.